International Journal of Energy Production and Management
https://www.acadlore.com/journals/IJEPM

Hydraulic Optimization and Headloss Modeling of the Penstock System in the Way Melesom Mini Hydropower Plant, Lampung, Indonesia

Nicco Plamonia[1,2*], Iik Nurul Ikhsan[1], Muhammad Rizky Darmawangsa[1], Iif Miftahul Ihsan[1], Ikhsan Budi Wahyono[1], Handy Chandra[1], Nana Sudiana[1], Nur Hidayat[1], Nicko Widiatmoko[3], Budi Kurniawan[3], Muhamad Komarudin[4], Rony Irawanto[1], Hadi Surachman[5], Hidir Tresnadi[3], Silvy Djayanti[1], Nyayu Fatimah Zahroh[6]

[1] Research Center for Environmental and Clean Technologies, National Research and Innovation Agency, 15314 South Tangerang, Indonesia
[2] Civil Engineering Department, Faculty of Engineering, Universitas Pancasila, 12640 Jakarta, Indonesia
[3] Research Center for Limnology and Water Resources, National Research and Innovation Agency, 10340 Jakarta, Indonesia
[4] Faculty of Engineering, National Science and Technology Institute, 12640 Jakarta, Indonesia
[5] Research Center for Energy Conversion and Conservation, National Research and Innovation Agency, 15134 South Tangerang, Indonesia
[6] Research Center for Climate and Atmosphere, National Research and Innovation Agency (BRIN), 15134 South Tangerang, Indonesia

[*] Correspondence: Nicco Plamonia1 (nicco.plamonia@brin.go.id)

Received: 11-25-2025 **Revised:** 01-14-2026 **Accepted:** 02-15-2026

Citation: N. Plamonia, I. N. Ikhsan, M. R. Darmawangsa, I. M. Ihsan, I. B. Wahyono, H. Chandra, N. Sudiana, N. Hidayat, N. Widiatmoko, B. Kurniawan, M. Komarudin, R. Irawanto, H. Surachman, H. Tresnadi, S. Djayanti, and N. F. Zahroh, "Hydraulic optimization and headloss modeling of the penstock system in the way melesom mini hydropower plant, Lampung, Indonesia," *Int. J. Energy Prod. Manag.*, vol. 11, no. 1, pp. 17–32, 2025. https://doi.org/10.56578/ijepm110102.

Abstract: Mini hydropower plants (MHPs) play a vital role in providing sustainable electricity to off-grid rural communities in Indonesia. This study optimizes the hydraulic performance of the penstock system for the Way Melesom MHP in Pesisir Barat, Lampung. Using a conservative design discharge of 0.822 m^3/s, derived from the F.J. Mock rainfall–runoff model and Flow Duration Curve (Q_{70}) analysis, hydraulic modeling was conducted using the Darcy–Weisbach and Hazen–Williams equations for four pipe diameters (DN400–DN700). The results show that increasing the pipe diameter reduces headloss and increases net head and power output, with diminishing efficiency gains beyond DN600. The DN600 configuration achieves an optimal balance—yielding a velocity of 2.91 m/s, headloss of 3.45 m, and a net head of 61.81 m, corresponding to an estimated output of 0.45 MW (2.76 GWh/year). This capacity can supply electricity to approximately 2,300 rural households, or up to 3,000 customers (450 VA each), supporting 10–12 small villages under an off-grid distribution network. The analysis confirms that DN600 provides the best technical–economic trade-off, recovering 95% of the gross head (65.26 m) with 90% hydraulic efficiency. The study highlights the importance of integrating hydrological, hydraulic, and energy modeling for optimizing closed-conduit systems in small-scale hydropower, ensuring both engineering efficiency and sustainable rural electrification.

Keywords: Penstock optimization; Head loss modeling; Mini hydropower; Darcy–Weisbach; Hydraulic efficiency; Rural electrification

1 Introduction

As an archipelagic nation, Indonesia still has about 6,700 unelectrified villages without reliable electricity access [1, 2] ($\approx$ 1.3 million households or 6.5 million people). In this context, Mini hydropower plants (MHPs) remain a promising and dependable renewable solution, outperforming solar and gas systems in efficiency [3–7]. The performance of MHPs depends strongly on penstock hydraulics [8], which control energy transfer from intake

to turbine. Yet few studies have integrated flow analysis, headloss modeling, and power estimation—especially for closed-conduit systems [9–12].

Compared to previous research in Nepal and India, which primarily emphasizes discharge estimation and hydrological forecasting for run-of-river schemes, this study adopts a more integrated approach by coupling hydrological modeling and hydraulic optimization within a unified analytical framework. Such integration enables quantitative evaluation of efficiency trade-offs between headloss reduction and economic feasibility, particularly under humid tropical conditions where rainfall variability and steep topography strongly influence system performance. This comparative perspective highlights the methodological novelty and regional relevance of the present work for small hydropower applications in Indonesia and Southeast Asia.

This study addresses the gap by analyzing the Way Melesom MHP penstock using a coupled hydrological–hydraulic model to assess design discharge, headloss, and power output across multiple pipe diameters. Using both the Darcy–Weisbach and Hazen–Williams equations [9, 13–17].

Hopefully, This study fills that gap by coupling hydrological dependable-flow modeling with dual hydraulic loss equations (Darcy–Weisbach and Hazen–Williams) to optimize penstock design—a novel framework for Indonesian mini-hydropower.

The research question is: Which penstock diameter provides the optimal balance between hydraulic efficiency and power output under site-specific conditions? Using steady-state analysis, headloss and energy output were modeled for several diameters based on design discharge derived from F.J. Mock and NRECA methods [18, 19]. Scientifically, this study advances closed-conduit flow modeling for small hydropower; practically, it supports sustainable rural electrification through optimized penstock design that maximizes efficiency with minimal losses [20–22].

The hypothesis is that "Increasing pipe diameter decreases frictional headloss and increases power output up to an optimal threshold". beyond which efficiency gains become negligible." Beyond hydraulic efficiency, economic feasibility plays a critical role in penstock optimization. In small-scale hydropower systems, even marginal improvements in hydraulic performance must be justified against material and installation costs, which often dominate total project expenses. Therefore, this study not only analyzes the hydraulic performance of the penstock but also evaluates the cost–benefit sensitivity among different pipe diameters to determine the most economically optimal configuration for the Way Melesom MHP.

2 Methods

The Methods section is organized systematically, covering site description; (Section 2.1), penstock design parameter (section 2.2), headloss modeling (section 2.3), net head power output estimation (section 2.4), surge transient (2.5), eficiency refinement (section 2.6), economic sensitivity (section 2.7), and the conceptual framework (2.8). this structure hopefully provides a coherent workflow linking field conditions, hydrological analysis, and hydraulic optimization of the penstock system. The overall research workflow is illustrated in Figure 1, which connects the hydrological, hydraulic, and economic components of the analysis.

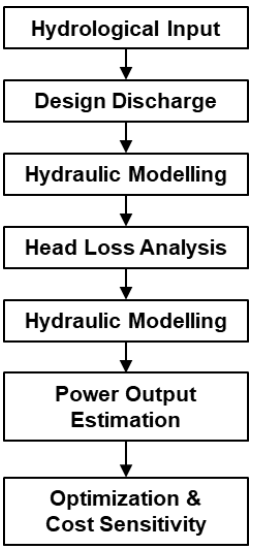

Figure 1. Workflow

The process begins with rainfall–runoff modeling and dependable flow estimation, continues through hydraulic simulation and headloss evaluation, and concludes with power output estimation and cost–benefit optimization.

This framework ensures methodological consistency and a clear logical transition across all subsections (2.1–2.7).

2.1 Site Description

The Way MHP is located in Bambang Village, Lemong District, Pesisir Barat Regency, Lampung Province, Indonesia (approximately 04°58'11.6"S; 103°45'22"E) (See Figure 2).

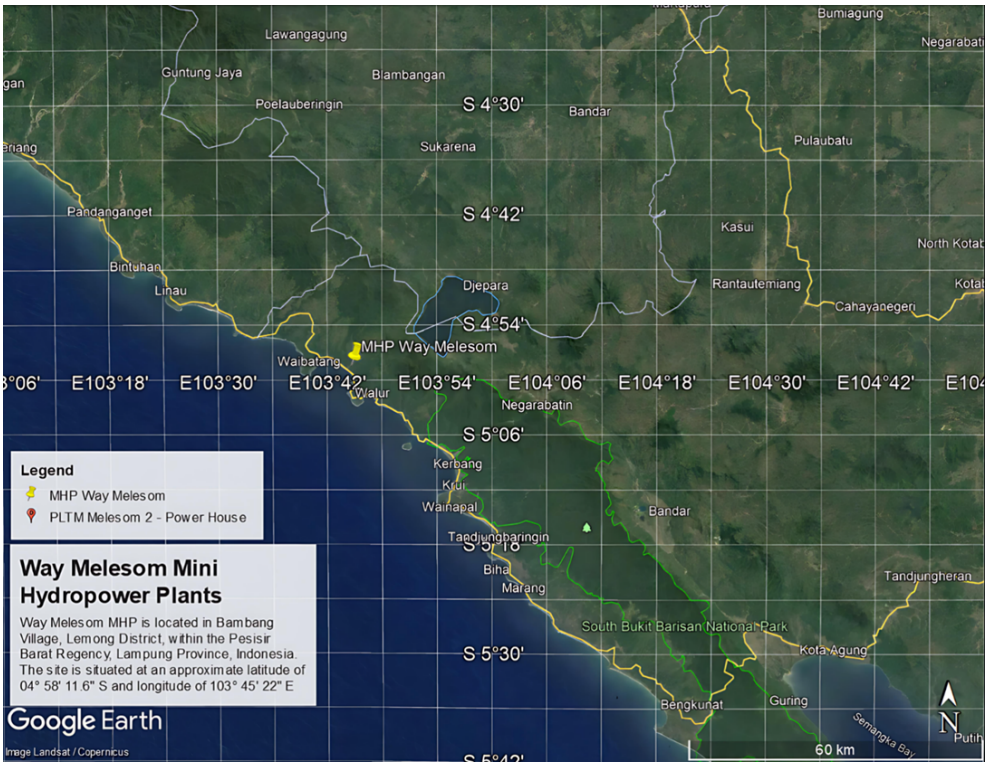

Figure 2. Way Melesom mini hydropower plants location (1)

The project supplies electricity to around 2,300 rural households and utilizes the hydrological potential of the 46.31 km^2 Melesom River catchment situated within the western coastal hills of southern Sumatra. The terrain is moderately to steeply hilly (8°–35°), allowing an efficient gravitational flow from the intake to the powerhouse through a short high-head penstock system.

The gross head between the forebay (275.5 m) and the tailwater (210.2 m) is approximately 65 m, with a total penstock length of 160 m. The longitudinal alignment—from the intake, headrace, and forebay to the powerhouse—is summarized in Table 1 and Figure 3 as follow. These site characteristics provide the physical basis for hydraulic modelling and energy estimation.

Table 1. Elevation profile and geographic coordinates of the penstock alignment

Station	Cumulative Distance (m)	Longitude (E)	Latitude (S)	Ground Elevation (m)	Pipe Centreline Elevation (m)	Description
0+000	0	10.375.258	–4.97036	∼ 278.0	∼ 276.5	Weir / Intake
0+050	50	10.374.600	–4.97200	∼ 272.0	∼ 269.5	Headrace Channel
0+100	100	10.374.244	–4.97428	275.5	274.0	Head pond / Forebay
0+160	160	10.374.153	–4.97500	210.2	209.0	Powerhouse

Dependable Flow and Design Discharge Estimation [11, 23, 24]. The dependable flow (Q_{70}) was derived from the Flow Duration Curve (FDC) constructed using Mock-simulated monthly runoff data, representing the discharge available 70% of the time in an average year. Field measurements at the site indicated a mean discharge of 3.44 m^3/s, which aligns with the simplified gross water balance estimation. Using the rainfall–area–time relationship (See Eq. (1)):

$$Q_{\text{dep}} = \frac{\sum(P \times A)}{T} \tag{1}$$

where, P = precipitation (m) = 3.281 m/year, A= catchment area (km^2) = 46.31 km^2 = 46,310,000 m^2, and T = time period (seconds per year) = 31,536,000 s, yields Q_{dep} = 4.81 m^3/s , representing the theoretical upper limit if all rainfall became direct runoff.

The Mock water-balance simulation produced a more realistic mean discharge of 1.54 m^3/s, confirming that infiltration and evapotranspiration were properly accounted for. From the FDC, the dependable flow at 70% exceedance was determined as Q_{70} = 4.02 m^3/s. For design purposes, a safety factor (SF = 4) was applied to obtain a conservative design discharge, see Eq. (2):

$$Q_{\text{design}} = Q_{70}/SF \tag{2}$$

where, Q_{design} serves as the hydrological basis for all subsequent penstock analyses (DN400–DN700), ensuring that the design remains technically robust and statistically consistent under site-specific hydrological conditions.

Following the determination of the design discharge, the next step defines the geometric and hydraulic parameters required for penstock analysis, linking the hydrological input to the mechanical design domain.

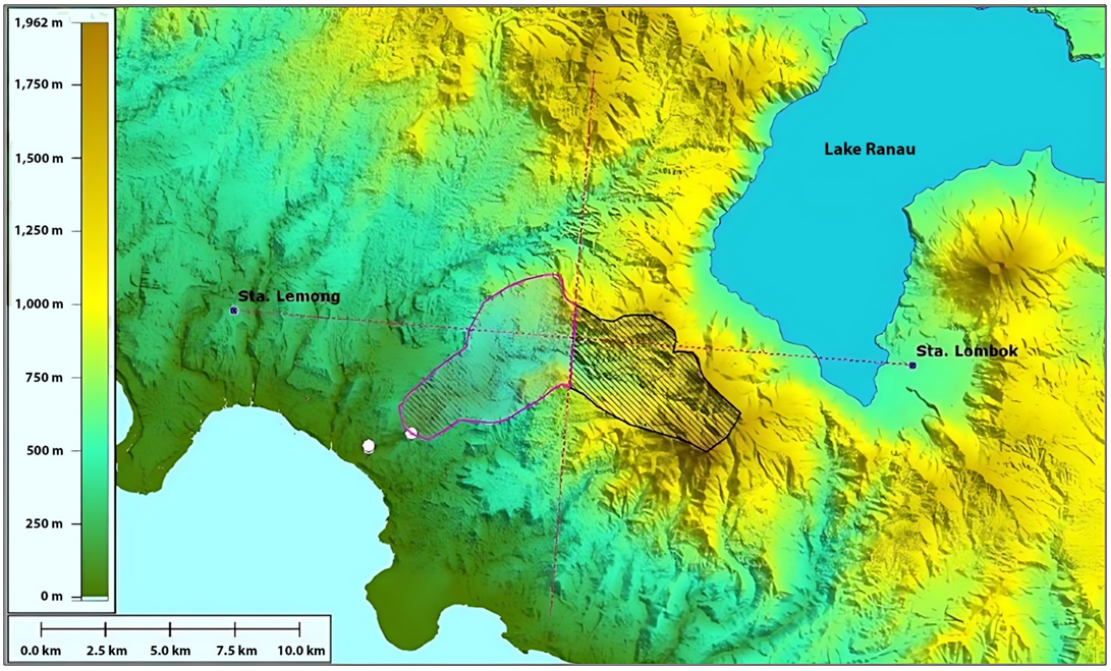

Figure 3. Way Melesom mini hydropower plants location (2)

2.2 Penstock Design Parameters

After defining the design discharge, the relevant hydrological parameters are summarized in Section 2.2.1. The subsequent analyses include the gross head determination (Section 2.2.1), penstock alignment description (Section 2.2.2), and evaluation of four pipe diameters—DN400, DN500, DN600, and DN700 (Section 2.2.3). Flow characteristics such as velocity, Reynolds number, and friction factor (Section 2.2.4) were then derived to assess energy transfer efficiency and head loss potential (Section 2.2.5). This stage integrates the hydrological modeling results with the hydraulic design process, providing the foundation for the subsequent head loss and power output analyses.

Having established the physical geometry, this subsection specifies the governing hydraulic parameters and constants used in modeling the flow behavior along the penstock.

2.2.1 Hydraulic modeling parameters

Fundamental assumptions and key parameters—covering hydrological inputs, topographic characteristics, and hydraulic constants (Table 2 to Table 4)—were established to ensure that the penstock modeling accurately represents

site-specific conditions for runoff estimation, head determination, and hydraulic performance analysis of the Way Melesom Mini Hydropower Plant.

Collectively, these parameters ensure that the hydraulic computations—including head loss, flow velocity, and power output—are grounded in consistent hydrological conditions, accurate site geometry, and standardized physical properties, thereby providing a reliable framework for penstock design and performance evaluation.

Table 2. Hydrological parameters

No.	Parameter	Symbol	Value	Unit	Description
1	Annual rainfall	P	3,281	mm/year	Derived from long-term rainfall records (Lemong and Lombok Stations), representing the mean hydrological input to the catchment.
2	Catchment area	A	46.31	km^2	Determined through topographic delineation (GIS) and field verification; used as basis for runoff and discharge estimation.
3	Field-measured discharge	Q_{field}	3.44	m^3/s	Mean discharge measured at the intake during April–May 2024 under natural flow conditions.
4	Dependable flow (70%)	Q_{70}	4.02	m^3/s	Discharge exceeded 70% of the time from the FDC based on Mock runoff simulation.
5	Design discharge	Q_{design}	0.822	m^3/s	Derived from Q_{70} with a safety factor (SF = 4); used for penstock hydraulic modelling.
6	Specific discharge	q	0.0177	$\mathrm{m}^3/(s{\cdot}\mathrm{km}^2)$	Discharge normalized by catchment area; represents runoff yield of the watershed.

Table 3. Topographic and geometric parameters

No.	Parameter	Symbol	Value	Unit	Description
1	Forebay elevation	Z_{f}	275.5	m	Obtained from detailed topographic survey at intake/headpond.
2	Powerhouse elevation	Z_{p}	210.2	m	Elevation of tailrace or turbine centreline.
3	Gross head	H_{gross}	65.26	m	Elevation difference between forebay (Z_{f}) and powerhouse (Z_{p}).
4	Penstock length	L	160	m	Based on surveyed alignment following the terrain profile.
5	Average slope	S	0.408	–	Dimensionless slope ratio (H_{gross}/L).
6	Slope (%)	–	40.8	%	Converted from dimensionless slope to percentage form.

Table 4. Hydraulic and physical constants

No.	Parameter	Symbol	Value	Unit	Description
1	Water density	ρ	1	kg/m^3	Standard freshwater density at $\sim 20^{\circ}\mathrm{C}$; used in power and head loss equations.
2	Gravitational acceleration	g	9.81	m/s^2	Physical constant applied in head and energy computations.
3	Kinematic viscosity	ν	1×10^{-6}	m^2/s	Represents viscosity of water at $\sim 20^{\circ}\mathrm{C}$; used for Reynolds number calculation.
4	Initial friction factor	f	0.03	–	Assumed for preliminary head loss in steel pipes under turbulent flow; refined using the Colebrook–White equation [25].
5	Turbine–generator efficiency	η	0.85	–	Combined mechanical and electrical efficiency typical for crossflow or Pelton turbines.

2.2.2 Gross head determination

Based on the topographic survey, the geometric and hydraulic parameters of the penstock are summarized in Table 3 above. The calculated slope of 40.8% indicates a steep hydraulic gradient along the 160 m alignment, enabling efficient gravitational flow toward the turbine. The gross head, representing the total elevation difference between the forebay and the powerhouse, is 65.26 m, providing the available head before accounting for friction and turbulence losses in subsequent analyses.

2.2.3 Penstock length and alignment

The penstock length (L) yielding a total length of 160 m. The selected route represents an optimal balance between hydraulic efficiency and constructability, then provides a favorable descent for efficient gravitational energy conversion.

2.2.4 Pipe diameter variants (DN400–DN700)

Four commercially available steel pipe diameters available were evaluated: DN400, DN500, DN600, and DN700. These options were selected to represent a realistic range of pipe sizes used in small hydropower applications while capturing the non-linear relationship between diameter and frictional loss. The cross-sectional area (A) and mean velocity (V) for each diameter were calculated using equation as follows:

$$A = \frac{\mu D^2}{4}, V = \frac{Q}{A} = \frac{4Q}{\mu D^2} \tag{3}$$

where, (1) D = Pipe Diameter (m); (2) A = Cross-sectional Area (m^2); (3) V = Flow Velocity (m/s); (4) Q = Design Discharge (m^3/s)

Design guidelines for micro-hydro penstocks recommend a flow velocity between 2–4 m/s to minimize frictional losses [5, 11], erosion, and cavitation while maintaining economical pipe sizing. Values below this range may lead to sediment deposition, whereas higher velocities can accelerate pipe wear and increase head loss.

2.2.5 Hydraulic properties (Reynolds number, velocity)

The Reynolds number (Re) was calculated to determine the flow regime within the penstock and to justify the use of turbulent-flow head loss models [26–28]. It is expressed as:

$$Re = \frac{VD}{v} \tag{4}$$

where, (1) V = mean flow velocity (m/s); (2) D = pipe diameter (m); (3) v = kinematic viscosity of water, taken as 11×10^{-6} m^2/s at approximately 20 °C.

For all evaluated diameters (DN400–DN700), the resulting Reynolds numbers exceeded 10^6, confirming fully turbulent flow conditions ($Re \gg 4000$). This validates the use of the Darcy–Weisbach equation and Colebrook–White formulation for friction factor estimation in subsequent head loss modelling.

2.2.6 Friction factor and assumptions

An initial baseline friction factor (f) of 0.03 was adopted, which is a reasonable approximation for turbulent flow in commercial steel pipes. The absolute roughness (ε) of steel was assumed to be 0.045 mm. For more precise analysis, the friction factor can be refined iteratively using the Colebrook–White equation [25, 29]:

$$\frac{1}{\sqrt{f}} = -20 \log_{10} \left(\frac{\varepsilon/D}{3.7} + \frac{2.51}{\mathrm{Re}\sqrt{f}} \right) \tag{5}$$

where, (1) f = Darcy–Weisbach friction factor (dimensionless); (2) ε = absolute roughness of the pipe wall (m); (3) D = pipe diameter (m); (4) Re = Reynolds number (dimensionless), representing flow regime.

Although Colebrook iteration is recommended for detailed or final design, in this study f = 0.03 was retained for sensitivity and comparative analysis among different pipe diameters.

With the hydraulic parameters defined, the analysis proceeds to quantify frictional energy losses using two established approaches: the Darcy–Weisbach and Hazen–Williams equations.

2.3 Head Loss Modeling

Head loss analysis was conducted to quantify the energy losses due to pipe friction, which directly influence the hydraulic efficiency of the penstock. To ensure both precision and comparability, two established empirical–analytical models were applied: the Darcy–Weisbach [30] equation as the primary method (Section 2.4.1), and the Hazen–William's equation as a secondary benchmark (2.4.2). The Darcy–Weisbach approach provides a physically based estimate suitable for turbulent flow and variable roughness conditions, while the Hazen–William's equation serves as a simplified empirical check to validate the overall results. Together, these models yield head loss values for each pipe diameter scenario, forming the analytical foundation for evaluating the penstock's hydraulic performance.

2.3.1 Darcy–Weisbach

The Darcy–Weisbach [30] equation was used as the primary analytical method for calculating head loss along the penstock, as it provides a physically based representation of frictional energy losses under turbulent flow conditions [31]. The general form of the equation is expressed as:

$$h_f^{DW} = f\frac{L}{D}\frac{V^2}{2g} \tag{6}$$

where, (1) h_f^{DW} = headloss according to the Darcy-Weisbach equation (m); (2) h_f: head loss (m); (3) f: friction factor; (4) L: pipe length (m); (5) D: pipe diameter (m); (6) V: flow velocity (m/s); (7) g: gravity (9.81 m/s^2).

Darcy–Weisbach equation can also be expressed in expanded form as:

$$h_f = f \times \frac{L \times V^2}{2gD} \tag{7}$$

This formulation demonstrates that head loss increases proportionally with pipe length and the square of flow velocity, while it decreases with larger pipe diameter and lower friction factor. The Darcy–Weisbach model is therefore particularly suitable for turbulent flow conditions where the effects of pipe roughness and Reynolds number are significant, making it the preferred approach for detailed hydraulic design and performance evaluation of the Melesom penstock.

2.3.2 Hazen–Williams

For comparative purposes, the Hazen–equation Williams [32, 33] was also applied to estimate headloss empirically. This approach is widely used in practical hydropower and water conveyance systems due to its simplicity, though it is less precise for fully turbulent or high-Reynolds-number conditions. The equation is expressed as:

$$h_f^{HW} = 10.67L\frac{Q^{1.852}}{C^{1.852}D^{4.87}} \tag{8}$$

where, (1) h_f^{HW} = head loss calculated by the Hazen-Williams method (m); (2) f = friction constant; (3) Q = flow (m^3/s); (4) L = lenght (m); (5) D: pipe diameter (m); (6) C = Hazen-Williams roughness coefficient (dimensionless), taken as 120 for commercial steel pipes:

$$h_f = 10.67 \cdot \frac{L}{C^{1.852}} \cdot \frac{Q^{1.852}}{D^{4.87}} \tag{9}$$

The resulting value h_f^{HW} represents the head loss along the penstock wall in meters of water column (m). While the Darcy-Weisbach model remains the preferred approach for turbulent flow conditions and when the effect of pipe roughness (ε/D) is significant, the Hazen-William's method was retained here as a sanity check to validate the overall magnitude of head loss estimates and ensure model consistency.

The computed head losses are then applied to determine the effective net head, forming the basis for estimating power output and overall system efficiency.

2.4 Net Head and Power Output Estimation

This section establishes the relationship between hydraulic losses and the effective energy delivered to the turbine. After determining the gross head and headlosses along the penstock, the net head (H_{net}) represents the usable hydraulic head available for power generation [25, 34].

$$H_{net} = H_{gross} - h_f \times \eta \tag{10}$$

where, (1) H_{net} = net head available for power generation (m); (2) H_{gross} = gross head or total elevation difference between forebay and powerhouse (m); (3) h_f = total head loss due to pipe friction and minor losses (m).

Net Head is fundamental in quantifying the overall efficiency of the system, as it directly influences the power output and determines how effectively the penstock transfers potential energy into mechanical energy at the turbine shaft. To ensure operational safety under variable flow conditions, surge and transient analyses are conducted to evaluate potential pressure fluctuations along the penstock.

Power Output Estimation (P) [34]

$$P = \rho \times \mathrm{g} \times Q \times h_f \times \eta \tag{11}$$

where, P = power generated (Watt/KiloWatt/KVA); ρ = density of the fluid (kg/m^3); Q = volumetric flow rate (m^3/s); h_f = head loss (m); η = Turbine-generator efficiency (0–1), dimensionless.

2.5 Surge (Transient)

Surge or transient flow analysis was also considered to assess the potential for water hammer effects that may occur during rapid flow changes, such as valve closure or sudden turbine shutdown. A simplified Joukowsky formulation was used for preliminary evaluation [35]. Using the Joukowsky equation:

$$\Delta H = \frac{a \Delta V}{q} \tag{12}$$

where, (1) ΔH = transient head rise (m); (2) a = wave velocity in the pipe material and fluid (m/s); (3) ΔV = change in flow velocity during valve closure or turbine shutdown (m/s); (4) g: gravitational acceleration (9.81 m/s^2).

With a typical wave velocity of a = 1000 m/s (steel pipe), an instantaneous valve closure would generate surge heads of approximately ΔH = 296.5 m (DN600) and ΔH = 217.8 m (DN700)-equivalent to 4–5 times the gross head. While these represent theoretical upper limits, controlled valve closure (5–10 s) can reduce surge pressures to within 1.5 × H_{gross}, maintaining pipe stresses within safe design margins. Refinement of the friction factor using the Colebrook-White formulation is introduced to improve model accuracy and assess sensitivity under turbulent flow conditions [25, 34].

2.6 Efficiency Refinement

To validate the robustness of the model, the friction factor (f) was refined using the Colebrook–White equation [32, 36], which accounts for pipe roughness and flow regime, See Eq. (5), where ε = 0.045 mm (steel pipe roughness).

2.7 Economic Sensitivity Framework

To complement the hydraulic performance modeling, a simplified cost–benefit assessment was carried out to quantify the relationship between power gain and material cost for each pipe diameter. The analysis considers unit pipe cost (USD/m), installation cost factor (20% of material cost), and estimated energy output (kWh/year) derived from the net head and discharge calculations. The economic sensitivity index (ESI) was defined as:

$$ESI = \frac{\Delta P / P_{ref}}{\Delta C / C_{ref}} \tag{13}$$

where, $\Delta P / P_{ref}$ represents the relative gain in power output compared to the reference diameter (DN600), and $\Delta C / C_{ref}$ represents the relative increase in total cost. An ESI < 1 indicates an economically inefficient design, as the power gain is smaller than the proportional increase in cost.

Cost data were estimated from regional supplier quotations (2024) for steel penstocks of 400–700 mm diameters (unit cost $\approx$ USD 450–610 per meter). The DN600 configuration served as the reference case for both hydraulic and economic comparisons.

Finally, the hydraulic results are coupled with a cost–benefit evaluation to determine the most economically feasible penstock diameter, completing the optimization workflow introduced in Figure 1.

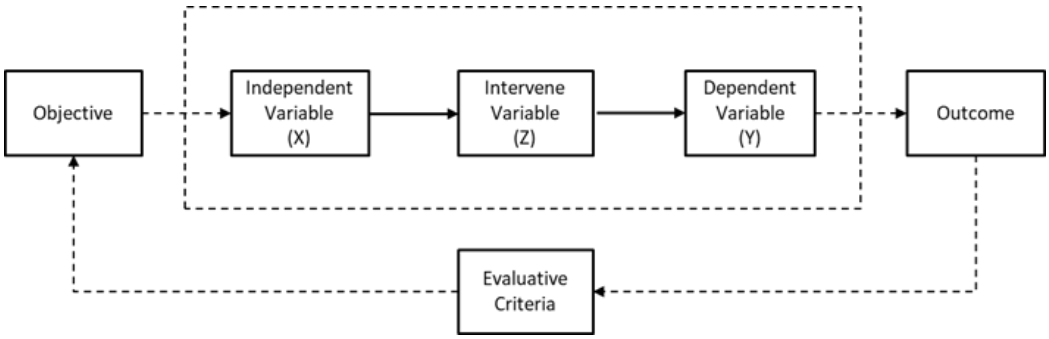

Figure 4. Conceptual model

2.8 Conceptual Model

The conceptual framework in Figure 4 illustrates the relationship between pipediameter (∅), head loss (h_f), net head (H_{net}), and power output (P), showing how these hydraulic parameters interact to determine the overall system performance.

The independent variable, pipe diameter (DN), directly affects flow velocity and frictional losses. Larger diameters reduce friction and improve flow efficiency, but increase cost. Four commercial diameters—DN400, DN500, DN600, and DN700—were evaluated to capture the non-linear relationship between diameter and head loss.

The intervening variables consist of: (1) head loss (h_f), representing energy loss due to friction along the penstock; and (2) net head (H_{net}), the effective head available after subtracting head loss from the gross head. Both are direct outcomes of pipe diameter and determine hydraulic efficiency.

The dependent variable, power output (P), represents the electrical energy generated based on net head, discharge, and turbine efficiency. Higher (H_{net}) and lower h_f result in greater P.

The evaluative criterion, system performance, measures how effectively the penstock converts hydraulic potential into power. Positive performance (+) indicates efficient operation with minimal losses, while negative (–) reflects underperformance due to high head loss or poor diameter selection.

Output Indicators are the specific measurable outcomes that reflect the system's performance. Based on System Performance, the key indicators include pipe diameter, head loss, net head, power output, and flow rate. These variables and their roles within the evaluative framework are summarized in Table 5, here's how Outcome Indicators would work: (1) Power Output (P): If the power output is high, this would indicate positive performance. If it's low, it suggests negative performance, potentially due to factors like inappropriate pipe diameter or inefficiencies in flow; (2) Head loss (h_f): If headloss is minimized, performance is positive. High head loss indicates poor design or operational inefficiency, leading to negative performance; (3) Net Head (H_{net}): The greater the net head, the better the system's performance, contributing to a positive result. Lower net head means the system is less efficient and could be rated negative.

Table 5. The output indicators

Evaluative Criteria	Variable	No	Outcome Indicator	Unit
(-) or (+)	Independent	1	Diameter (∅)	m
	Intervening	1	Head loss (h_{f})	m
		2	Net head (H_{net})	m
	Dependent	1	Power output (P)	kW
		2	Flow rate (Q)	m^3/s

3 Results

3.1 Longitudinal Profile

Figure 5 illustrates the longitudinal profile of the penstock for the Way Melesom MHP. The alignment extends approximately 160 meters from the forebay to the powerhouse, following the natural terrain slope. The penstock has been redesigned with a nominal diameter of 0.6 meters (DN600), selected as the most hydraulically efficient and economically viable configuration according to the optimization analysis. The alignment includes four major anchor blocks (AB-01 to AB-04) to ensure structural stability against internal pressure and external loads, particularly given the steep slope of about 40.8%.

As shown in the longitudinal section, the penstock begins at the intake structure near elevation +275.5 m and terminates at the powerhouse around +210.2 m, yielding a gross head of approximately 65 m. The consistent 0.6 m diameter ensures uniform velocity and reduced frictional losses throughout the conduit, while the anchor block placements maintain hydraulic and structural safety along the steep descent. This configuration supports stable flow conveyance toward the turbine and forms the geometric foundation for the hydraulic modeling and headloss analysis discussed in subsequent sections.

3.2 Hydraulic Results by Pipe Diameter

The evaluation of hydraulic and energy performance across four penstock diameters (DN400–DN700) was conducted to identify the configuration that provides the best balance between hydraulic efficiency, power output.

The resulting values of flow velocity (V), headloss (h_f), net head (H_{net}), and power output (P) were assessed and categorized as negative, moderate, or positive in terms of overall system performance. The comparative results are presented in Table 6, summarizing the evaluative criteria and outcome indicators for each variable and performance parameter used in the hydraulic optimization of the Way Melesom penstock.

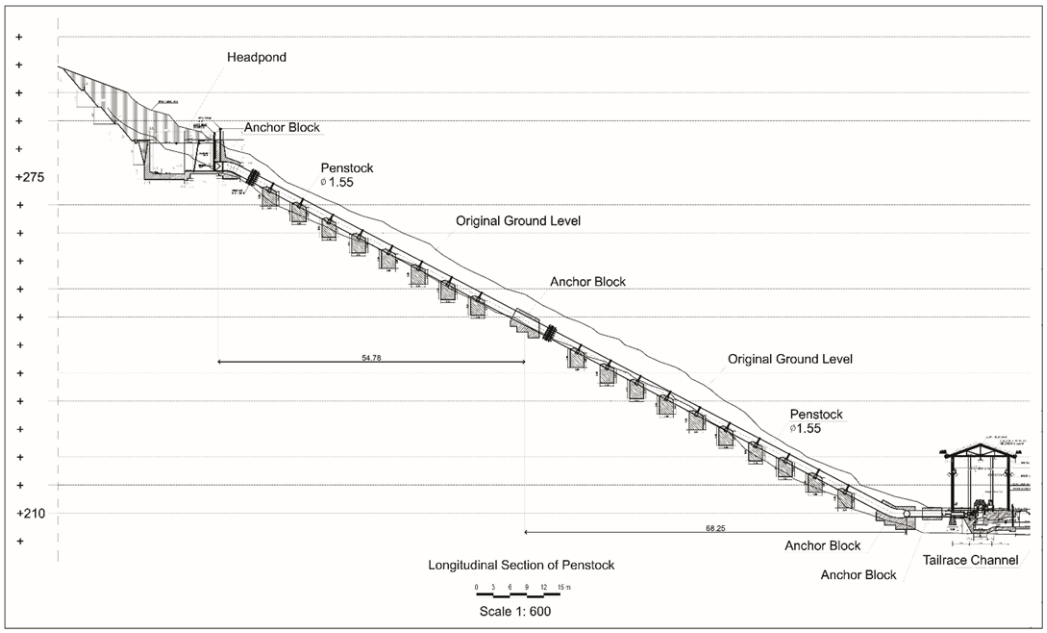

Figure 5. Penstock design

The Head loss calculations were performed using Darcy–Weisbach (primary) and Hazen–Williams (comparative). Hydraulic efficiency $\eta = 0.90$ assumed. Table 6 summarizes the hydraulic and energy parameters calculated for each penstock diameter. The results illustrate how pipe size affects flow velocity, head loss, and power output.

Table 6. Head loss, net head, and power output for tested diameters (Q_{design} = 0.822 m^3/s, L = 160 m: f = 0.030, C = 120)

Type	D (m)	A (m^2)	V (m/s)	Re (–)	$\frac{V^2}{2g}$ (m)	$h_{\text{f}}^{(\text{DW})}$ (m)	$h_{\text{f}}^{(\text{HW})}$ (m)	H_{net} (m)	P_{loss} (kW)	P (kW)
DN400	0.400	0.12566	6.541	2.62×10^6	2.181	26.17	14.52	39.09	211.03	283.69
DN500	0.500	0.19635	4.186	2.09×10^6	0.893	8.58	4.90	56.68	69.20	411.41
DN600	0.600	0.28274	2.907	1.74×10^6	0.431	3.45	2.02	61.81	27.79	448.61
DN700	0.700	0.38485	2.136	1.50×10^6	0.233	1.59	0.95	63.67	12.86	462.05

3.3 Worked Example for DN600

As an illustrative case, the following calculation demonstrates the derivation of hydraulic parameters for the DN600 configuration (design discharge = 0.822 m^3/s):

$$A = \frac{\mu D^2}{4} = \frac{\mu (0.6)^2}{4} = 0.283 \text{ m}^2 \tag{14}$$

Eq. (3) defines the pipe's cross-sectional area (A) as a function of its internal diameter (D). For DN600, this yields an effective flow area of approximately 0.283 m^2.

$$V = \frac{Q}{A} = \frac{0.822\ \mathrm{m}^3/\mathrm{s}}{0.283 m^2} = 2.91\ \mathrm{m/s} \tag{15}$$

According to the continuity relation (rearranging Eq. (3)), the mean flow velocity (V) is obtained by dividing the discharge by the cross-sectional area. The calculated velocity (2.91 m/s) lies within the recommended design range of 2–4 m/s for mini-hydropower penstocks, ensuring stable flow without excessive friction or cavitation.

$$Re = \frac{VD}{v} = \frac{2.91.0.6}{1 \times 10^{-6}} = 1.74 \times 10^6 \tag{16}$$

Following Eq. (4), the Reynolds number (Re) confirms the flow regime inside the pipe. The computed Re $\approx$ 1.7 × $10^6 \gg$ 4000 indicates fully turbulent flow, validating the use of turbulent-flow head loss models (Darcy–Weisbach and Colebrook–White).

$$h_f^{DW} = f\frac{L}{D}\frac{V^2}{2g} = 0.03\frac{160}{0.6}\frac{(2.91)^2}{2.9.8} = 3.45\ \mathrm{m} \tag{17}$$

Finally, applying the Darcy–Weisbach equation (Eq. (17)) with a friction factor (f = 0.03), a pipe length (L = 160 m), and gravitational acceleration (g = 9.81 m/s^2), the head loss (h_x) for DN600 is obtained as 3.45 m.

This head loss value matches the result presented in Table 6, confirming consistency between analytical formulation and tabulated computation. The stepwise derivation also illustrates the physical relationships among discharge, velocity, and energy loss, providing a transparent link between the governing equations and the final hydraulic results used for system optimization.

To complement the quantitative results, Table 7 provides a qualitative evaluation of the hydraulic performance for each pipe diameter (DN400–DN700). The table integrates the independent (diameter), intervening (head loss and net head), and dependent (power output) variables, together with their performance classification and interpretation. This assessment highlights how system efficiency and energy recovery improve with increasing pipe diameter until an optimal point is reached at DN600, beyond which performance gains become marginal compared to cost escalation.

Table 7. Qualitative evaluation of system performance for each diameter

Independent		**Intervening**		**Dependent**		**Performance**	**Evaluation**	**System Performance Interpretation**
DN (m)	**V (m/s)**	**h_f (m)**	**H_{net} (m)**	**P (kW)**	**Q (m^3/s)**			
DN400	6.54	26.17	39.09	283.7	0.822	Negative (–)	High velocity and excessive energy loss; poor efficiency.	Very high flow velocity causes excessive frictional losses, significantly reducing efficiency and power output.
DN500	4.19	8.58	56.68	411.4	0.822	Moderate (+/–)	Acceptable hydraulically but close to the upper design velocity.	Moderate flow velocity and frictional loss; efficiency improved but not optimal.
DN600	2.91	3.45	61.81	448.6	0.822	Positive (+)	Optimal efficiency and stable operation; recommended configuration.	Ideal velocity (2–4 m/s) with low head loss (3.45 m) and 95% gross head recovery → optimal technical–economic balance.
DN700	2.14	1.59	63.67	462.0	0.822	Positive (+)	Hydraulically superior, but economically inefficient.	Very low head loss and highest power output, but only 3% gain compared to DN600; increased material cost [37] makes it less feasible.

3.4 Analysis of Intervening Variables

The analysis revealed that DN400 exhibits the poorest hydraulic performance, with a high flow velocity of 6.54 m/s causing excessive head loss (26.17 m), which reduces the net head to 39.09 m and results in a power output of $\approx$ 283.7 kW. This velocity exceeds the recommended design limit ($>$ 4 m/s), creating a risk of erosion and abrasion along pipe joints, thus rendering DN400 unsuitable for sustained operation.

A moderate improvement is observed with DN500, where head loss is reduced to 8.58 m, yielding a net head of 56.68 m and a power output of $\approx$ 411.4 kW. However, its velocity of 4.19 m/s remains close to the design threshold, suggesting the need for additional erosion protection at bends and fittings.

The DN600 configuration represents the most balanced and optimal design, achieving an ideal velocity of 2.91 m/s, minimal head loss (3.45 m), and a power output of $\approx$ 448.6 kW. This configuration ensures high hydraulic efficiency, stable operation, and reasonable material cost.

Finally, DN700 achieves the lowest head loss (1.59 m) and highest output ($\approx$ 462.0 kW), yet the marginal gain of only 3% compared to DN600 does not justify the significantly higher construction cost—especially given the hilly terrain at the Way Melesom site.

Overall, head loss decreases non-linearly with increasing diameter, stabilizing beyond DN600, while net head shows a corresponding increase approaching the gross head limit. This confirms the diminishing-returns effect of enlarging pipe diameter in hydraulic systems.

3.5 Energy Performance and System Evaluation

The system performance improves consistently with increasing pipe diameter, primarily due to reduced frictional energy losses and the resulting increase in effective head. The relationship among the variables can be expressed as

$$\begin{aligned} &\text{DN} \uparrow \Rightarrow \text{ Velocity } \downarrow \Rightarrow \text{ Head Loss } \downarrow \\ &\Rightarrow \text{ Net Head } \uparrow \Rightarrow \text{ Power Output } \uparrow \end{aligned}$$

However, the benefit curve flattens beyond DN600, where the incremental power gain becomes insignificant relative to the increase in pipe cost. The intervening variables—head loss (h_f) and net head (H_{net})—show strong inverse and proportional correlations, respectively, validating the theoretical hydraulic model applied.

Among all configurations, DN600 provides the most favourable trade-off between technical efficiency and economic feasibility. It maintains an ideal flow velocity (2.9 m/s), low head loss (3.45 m), and high net head utilization (95% of the gross head), producing $\approx$ 448.6 kW of power with an overall hydraulic efficiency near 90%.

Thus, the DN600 steel penstock is identified as the optimal configuration, combining stable operation, efficient energy conversion, and long-term structural reliability for the Way Melesom Mini Hydro Power Plant.

3.6 Summary of System Performance

The performance classification—negative (DN400), moderate (DN500), and positive (DN600–DN700)—confirms that system efficiency increases with pipe diameter up to DN600, after which the improvement becomes marginal.

The DN600 configuration achieves 95% head recovery and approximately 90% hydraulic efficiency, offering the best balance between technical and economic considerations. While DN700 provides slightly higher hydraulic performance, its higher material and transportation costs make it less feasible for the project's scale and terrain conditions.

Table 8. Comparative cost–benefit assessment for penstock diameters

Diameter	Unit Cost (USD/m)	Total Cost (USD)	Power Output (kW)	Power Gain (%)	Cost Increase (%)	ESI ($\Delta P/\Delta C$)	Evaluation
DN400	360	57,600	283.7	–36.8	–20.0	1.84	Undersized, hydraulically inefficient
DN500	420	67,200	411.4	–8.3	–6.7	1.24	Acceptable, but close to limit
DN600	450	72,000	448.6	Reference (0)	Reference (0)	1.00	Optimal baseline configuration
DN700	610	97,600	462.0	+3.0	+35.6	0.08	Hydraulically superior but economically inefficient

3.7 Economic Sensitivity Analysis

In addition to the hydraulic evaluation, an economic sensitivity analysis was performed to compare the cost–performance trade-offs among the tested diameters. Table 8 summarizes the relative cost per meter, total pipe investment, annual energy output, and cost–benefit ratio.

The results reveal that while DN700 yields a 3% increase in power output compared to DN600, its cost rises by over 30%. The resulting ESI ≈ 0.08 indicates poor economic efficiency. Therefore, DN600 achieves the optimal balance between hydraulic performance and construction cost, maximizing power recovery without excessive capital expenditure.

This finding corroborates the diminishing-returns principle observed in the hydraulic domain, confirming that beyond a certain diameter threshold, additional energy gain no longer compensates for the exponential rise in material cost.

4 Discussion

4.1 Head lLoss and Hydraulic Efficiency

The results confirm a strong inverse correlation between pipe diameter and head loss, consistent with theoretical expectations. The DN400 configuration exhibits excessive frictional losses (26.17 m), resulting in low effective head utilization. In contrast, DN500 and DN600 progressively reduce head loss, improving flow stability and energy recovery.

Among all configurations, DN600 achieves near-optimal hydraulic efficiency, maintaining an ideal velocity range (2–4 m/s), minimal head loss (3.45 m), and high net head utilization (61.81 m), recovering about 95% of the gross head. This configuration offers the best balance between energy conversion and system economy.

While DN700 provides the lowest head loss (1.59 m), the hydraulic gain of only 3% over DN600 is offset by a ¿30% increase in material and transport costs, especially in the steep terrain of Way Melesom. Thus, DN600 marks the threshold of diminishing returns, where further diameter increases yield minor hydraulic benefits but significant economic penalties.

These findings confirm the diminishing-return relationship between pipe diameter and hydraulic efficiency [31], who demonstrated that increasing conduit diameter reduces headloss non-linearly until an economic optimum is reached. The hydraulic and energy efficiencies in pressurized water systems tend to plateau beyond a critical diameter due to cost escalation [15].

Hydraulic–economic trade-off principle in energy-distribution design for Indonesia's new capital, underscoring that performance optimization must integrate both fluid-mechanical and cost parameters [7].

Together, these comparisons strengthen the analytical depth of this study, showing that the Way Melesom DN600 configuration conforms with established optimization theory linking energy recovery and economic feasibility in small-scale hydropower systems.

4.2 Power Output and Design Trade-offs

Power output correlates directly with the effective head, increasing from 283.7 kW (DN400) to 462.0 kW (DN700). However, the incremental 3% gain from DN700 is economically unjustified given its 35% higher cost (USD 610 $\mathrm{m}-1$ vs USD 450 $\mathrm{m}-1$ for DN600).

When normalized by lifetime energy production, DN700's cost of energy (USD/kWh) is approximately 25% higher than DN600's.

Accordingly, DN600 represents the most technically efficient and economically viable configuration, ensuring stable energy delivery, low maintenance risk, and favorable long-term performance.

This confirms the design hypothesis that the optimal penstock diameter lies at the balance point between hydraulic efficiency and cost feasibility, a principle verified by both hydraulic and economic sensitivity analyses.

4.3 Efficiency Refinement

For DN600, the refined model increased net head from 61.8 m to ≈ 63.8 m and power output from 448.6 kW to ≈ 463.1 kW.

These results confirm that the initial design was conservative and that DN600 remains hydraulically optimal even under refined turbulent flow conditions. Presenting both assumed and refined friction cases strengthens design transparency and enables sensitivity analysis for future audits and optimization.

Refinement using the Colebrook–White equation reduced friction factors to $f \approx 0.0125$–0.0129, corresponding to 60–70% lower head loss than the initial assumption ($f = 0.03$). For DN600, the refined model increased the net head from 61.8 m to ≈ 63.8 m and power output from 448.6 kW to ≈ 463.1 kW. These findings confirm that the initial design was conservative and that DN600 remains hydraulically optimal even under refined turbulent-flow conditions. Presenting both cases improves transparency and supports sensitivity analyses for future optimization.

4.4 Surge and Operational Safety

Although the penstock is short (160 m) and conveys moderate discharge (0.822 m^3/s), the 65 m gross head warrants consideration of transient effects. Joukowsky analysis indicated that controlled valve closures ($\geq$ 5 s) maintain surge heads within 1.5 × H_{gross}, ensuring structural safety.

This highlights that the optimized DN600 not only achieves high hydraulic efficiency but also ensures operational reliability under transient conditions. The configuration provides sufficient structural resistance against pressure surges, minimizing risks of fatigue and cavitation during load variations or turbine shutdowns.

Therefore, the DN600 system represents a balanced design that combines steady-state efficiency, surge safety, and long-term durability, confirming its suitability for the steep and high-head environment of the Way Melesom Mini Hydropower Plant.

5 Conclusion

This study demonstrates that the DN600 steel penstock provides the most favorable balance between hydraulic performance, cost efficiency, and structural feasibility for the Way Melesom Mini Hydropower Plant.

By integrating hydrological simulation, hydraulic modeling, and economic sensitivity analysis, the research confirms that increasing diameter beyond DN600 yields diminishing hydraulic returns while substantially escalating project costs.

The DN600 configuration ensures reliable operation within the ideal velocity range (2–4 m/s), maintains approximately 95% head recovery, and supports efficient energy conversion with moderate construction investment.

Its cost–benefit ratio outperforms DN700, offering nearly identical power output at significantly lower cost, making it the technical–economic optimum for the site's terrain and budget constraints. In addition to achieving optimal hydraulic efficiency, DN600 also demonstrates the best economic performance, producing nearly the same power as DN700 but at substantially lower cost (USD 450 $m-1$ versus USD 610 m^{-1}). This confirms DN600 as the most cost-effective configuration for sustainable implementation under the budgetary limitations typical of rural mini-hydropower projects.

Overall, the analysis reinforces the principle that hydraulic optimization in small hydropower systems must be integrated with economic feasibility assessment.

The methodological framework developed in this study can guide future MHP designs in Indonesia and other regions with similar topographic and financial limitations—ensuring sustainable, efficient, and affordable rural electrification.

Future studies should include transient-flow and life-cycle cost analysis to extend this steady-state model toward dynamic optimization.

6 Recommendation

For the Way Melesom MHP, DN600 is recommended as the most efficient and cost-effective penstock configuration, offering an optimal balance between hydraulic performance and material feasibility. To enhance system stability and protect against transient pressures, several operational and structural measures are recommended. These include implementing controlled turbine shut-off sequences to prevent sudden velocity changes, installing air or vacuum valves at critical high points and downstream sections to relieve pressure fluctuations, and considering a small surge tank or standpipe near the powerhouse if numerical transient modeling indicates pressure peaks exceeding allowable limits. Additionally, it is essential to verify pipe wall thickness, anchoring systems, and structural supports to ensure resistance against short-term dynamic loads. The refined friction factor derived from the Colebrook analysis further improves the accuracy of damping coefficients in transient simulations, effectively linking steady-state headloss characteristics to the system's dynamic surge response.

Author Contribution

Conceptualization and methodology: N.P., I.N.I., and M.R.D.; Investigation and data analysis: I.M.I., I.B.W., H.C., N.S., and N.H.; Hydrological modeling and technical validation: N.W., B.K., and H.T.; Field survey and visualization: M.K., R.I., and H.S.; Editing, discussion, and review: S.D. and N.F.Z.; Supervision and final manuscript approval: N.P..

Acknowledgment

The authors would like to acknowledge the contributions of the PLTMH Melesom design team and PT. Graha Hidro Nusantara.

Data Availability

The data used to support the findings of this study are available from the corresponding author upon request.

Conflicts of Interest

The authors declare that they have no conflicts of interest.

References

[1] A. Syauqi, Y. W. Pratama, and W. W. Purwanto, "Sustainable energy system in the archipelagic country: Challenges and opportunities," in *Energy Systems Evaluation*. Springer, 2021, pp. 49–69. https://doi.org/10.1007/978-3-030-67529-5_3

[2] Y. Mohsin, "Archipelagic networks of power: Village electrification, politics, ideology, and dual national identity in Indonesia (1966-1998)," Ph.D. dissertation, Cornell University, 2015. https://ecommons.cornell.edu/bitstream/1813/39438/1/ysm5.pdf

[3] A. Mezzanotte, "Planning of rural electrification with mini-hydro-power systems in the Cimitarra basin (Colombia)," Master's thesis, Politecnico di Milano, 2017. https://www.politesi.polimi.it/handle/10589/146795

[4] A. Shrestha, Y. Rajbhandari, N. Khadka, A. Bista, A. Marahatta, and R. Dahal, "Status of micro/mini-grid systems in a himalayan nation: A comprehensive review," *IEEE Access*, vol. 8, pp. 120 983–120 998, 2020. https://doi.org/10.1109/ACCESS.2020.3006912

[5] O. Paish, "Small hydro power: Technology and current status," *Renew. Sustain. Energy Rev.*, vol. 6, no. 6, pp. 537–556, 2002. https://doi.org/10.1016/S1364-0321(02)00006-0

[6] C. S. Kaunda, "Hydropower in the context of sustainable energy supply: A review of technologies and challenges," *Int. Sch. Res. Notices*, vol. 2012, no. 1, p. 730631, 2012. https://doi.org/10.5402/2012/730631

[7] M. F. A. Rahman, N. A. Kamal, J. Abdullah, E. Quaranta, and S. Shin, "Unlocking the potential of micro-hydropower in water distribution networks: A comprehensive systematic review for Malaysia's sustainable energy future," *Discov. Sustain.*, vol. 6, no. 1, p. 56, 2025. https://doi.org/10.1007/s43621-025-00818-5

[8] S. Cassano and F. Sossan, "Stress-informed control of medium- and high-head hydropower plants to reduce penstock fatigue," *Sustain. Energy Grids Netw.*, vol. 31, 2022. https://doi.org/10.1016/j.segan.2022.100688

[9] G. S. Springer, "A pipe-based, first approach to modeling closed conduit flow in caves," *J. Hydrol.*, vol. 289, no. 1–4, pp. 178–189, 2004. https://doi.org/10.1016/j.jhydrol.2003.11.020

[10] D. S. Miller, "Headlosses in closed conduit systems flowing full," in *Discharge Characteristics*. Routledge, 2017, pp. 152–216.

[11] C. S. Kaunda, C. Z. Kimambo, and T. K. Nielsen, "Hydropower in the context of sustainable energy supply: A review of technologies and challenges," *ISRN Renew. Energy*, vol. 2012, pp. 1–15, 2012. https://doi.org/10.5402/2012/730631

[12] E. Wicklein, "Hydraulic analysis and headworks," in *CFD Modelling for Wastewater Treatment Processes: IWA Working Group on Computational Fluid Dynamics*, 2022, pp. 37–50. https://doi.org/10.2166/9781780409030_0037

[13] L. Ormsbee and T. Walski, "Darcy-weisbach versus hazen-williams: No calm in west palm," in *World Environmental and Water Resources Congress 2016*, 2016, pp. 455–464. https://doi.org/10.1061/9780784479865.048

[14] J. D. Valiantzas, "Modified Hazen–Williams and Darcy–Weisbach equations for friction and local head losses along irrigation laterals," *J. Irrig. Drain. Eng.*, vol. 131, no. 4, pp. 342–350, 2005. https://doi.org/10.1061/(ASCE)0733-9437(2005)131:4(342)

[15] M. R. N. Vilanova and J. A. P. Balestieri, "Energy and hydraulic efficiency in conventional water supply systems," *Renew. Sustain. Energy Rev.*, vol. 30, pp. 701–714, 2014. https://doi.org/10.1016/j.rser.2013.11.024

[16] R. G. Allen, "Relating the Hazen-Williams and Darcy-Weisbach friction loss equations for pressurized irrigation," *Appl. Eng. Agric.*, vol. 12, no. 6, pp. 685–693, 1996. https://doi.org/10.13031/2013.25699

[17] R. Jamil and M. A. Mujeebu, "Empirical relation between Hazen-Williams and Darcy-Weisbach equations for cold and hot water flow in plastic pipes," *Water*, vol. 10, pp. 104–114, 2019. https://doi.org/10.14294/WATER.2019.1

[18] K. Beven, *Rainfall-Runoff Modelling: The Primer*. Wiley, 2012. https://doi.org/10.1002/9781119951001

[19] A. T. Juniati, N. Plamonia, D. Ariyani, M. Fitrah, and D. A. Kuncoro, "Landslide hazard mapping and bio-engineering solutions for riverbank stabilization in the Cisanggarung River Basin, Indonesia: A GIS-based approach," *J. Degrad. Min. Lands Manag.*, vol. 12, no. 3, pp. 7637–7648, 2025. https://doi.org/10.15243/jdmlm.2025.123.7637

[20] N. Plamonia, "Penstock pipe's hydraulic design for the mini hydropower plant at Besai Kemu, Bukit Kemuning, Lampung, Indonesia," *IOP Conf. Ser. Earth Environ. Sci.*, vol. 1388, p. 012057, 2024. https://doi.org/10.1088/1755-1315/1388/1/012057

[21] Y. S. Putraa, E. Noviani, and Muhardi, "Numerical study of the effect of penstock dimensions on a micro-hydro

system using a computational fluid dynamics approach," *Int. J. Renew. Energy Dev.*, vol. 11, no. 2, pp. 491–499, 2022. https://doi.org/10.14710/ijred.2022.42343

[22] M. Rumbayan and R. Rumbayan, "Feasibility study of a micro hydro power plant for rural electrification in Lalumpe Village, North Sulawesi, Indonesia," *Sustainability*, vol. 15, no. 19, p. 14285, 2023. https://doi.org/10.3390/su151914285

[23] A. Quader and Y. Guo, "Peak discharge estimation using analytical probabilistic and design storm approaches," *J. Hydrol. Eng.*, vol. 11, no. 1, pp. 46–54, 2006. https://doi.org/10.1061/(ASCE)1084-0699(2006)11:1(46)

[24] A. Petroselli, R. Piscopia, and S. Grimaldi, "Design discharge estimation in small and ungauged basins: EBA4SUB framework sensitivity analysis," *J. Agric. Eng.*, vol. 51, no. 2, pp. 107–118, 2020. https://doi.org/10.4081/jae.2020.1040

[25] C. F. Colebrook and C. M. White, "Experiments with fluid friction in roughened pipes," *Proc. R. Soc. London A*, vol. 161, no. 906, pp. 367–381, 1937. https://doi.org/10.1098/rspa.1937.0150

[26] Y. J. Moon, *Introduction to Fluid Dynamics: Understanding Fundamental Physics*. Wiley, 2022.

[27] F. M. White, *Fluid Mechanics*. McGraw Hill, 2011.

[28] Y. Cengel and J. Cimbala, *Fluid Mechanics Fundamentals and Applications*. McGraw-Hill, 2013. https://books.google.co.id/books?id=LIZvEAAAQBAJ

[29] L. F. Moody, "Friction factors for pipe flow," *J. Fluids Eng.*, vol. 66, no. 8, pp. 671–678, 1944. https://doi.org/10.1115/1.4018140

[30] B. E. Larock, R. W. Jeppson, and G. Z. Watters, *Hydraulics of Pipeline Systems*. CRC Press, 1999.

[31] K. Purohit, S. P. Harsha, and R. K. Purohit, *Fluid Mechanics*. Scientific Publishers, 2012.

[32] A. C. Twort, D. D. Ratnayaka, and M. J. Brandt, *Water Supply*. IWA Publishing, 2000.

[33] D. J. Stephenson, *Stormwater Hydrology and Drainage*. Elsevier, 1981.

[34] H. W. Coleman, C. Y. Wei, and J. E. Lindell, "Hydraulic design of spillways," in *Hydraulic Design Handbook*, 2004, pp. 17–41. https://doi.org/10.15243/jdmlm.2025.123.7637

[35] J. Swaffield, *Transient Airflow in Building Drainage Systems*. CRC Press, 2010.

[36] D. I. H. Barr, *Additional Tables for the Hydraulic Design of Pipes, Sewers and Channels*. Thomas Telford, 1993.

[37] R. A. Rahman, N. Plamonia, D. Setiawan, and R. D. D. Putra, "Development and thermal investigation of modified octadecanoic acid as energy storage material," *Chem. Chem. Technol.*, vol. 18, no. 4, pp. 615–622, 2024. https://doi.org/10.23939/CHCHT18.04.615

Nomenclature

A	Cross-sectional area of pipe, m^2
D	Internal pipe diameter, m
f	Darcy–Weisbach friction factor
g	Gravitational acceleration, $\mathrm{m/s}^2$
H_{gross}	Gross head (forebay – powerhouse), m
H_{net}	Net head after friction loss, m
h_{f}	Head loss due to pipe friction, m
L	Total penstock length, m
P	Power output, kW
Q	Flow discharge, m^3/s
Q_{70}	Dependable flow (available 70% of time), m^3/s
Q_{design}	Design discharge (Q_{70}/SF), m^3/s
Re	Reynolds number
S	Hydraulic slope ($= H/L$)
SF	Safety factor
V	Mean velocity in pipe, m/s
ρ	Density of water, $\mathrm{kg/m}^3$
ν	Kinematic viscosity of water, m^2/s
ε	Pipe wall roughness, m
η	Turbine–generator efficiency